Journal of The Electrochemical Society, **159** (9) A1405-A1409 (2012)
0013-4651/2012/159(9)/A1405/5/$28.00 © The Electrochemical Society

User-Friendly Differential Voltage Analysis Freeware for the Analysis of Degradation Mechanisms in Li-Ion Batteries

Hannah M. Dahn, A. J. Smith, J. C. Burns,* D. A. Stevens, and J. R. Dahn,z**

Department of Physics and Atmospheric Science, Dalhousie University, Halifax, Nova Scotia B3H 4R2, Canada

A user-friendly differential voltage analysis software has been developed and is described here. High-precision reference potential-specific capacity data for Li/negative electrode and Li/positive electrodes, as well as the cycled full cell potential-specific capacity, must be supplied by the user. From these, the differential voltage versus capacity, dV/dQ vs. Q, of a full Li-ion cell is calculated and compared to experiment. The calculated dV/dQ vs. Q curve has four adjustable parameters which are optimized manually with slider bars or automatically by least squares fitting of the calculation to experiment. The parameters are the positive electrode mass, the negative electrode mass, the positive electrode slippage and the negative electrode slippage. Examples of the use of the program are given for graphite/$LiCoO_2$ wound cells cycled for hundreds of cycles. The variation of the four parameters with cycle number give insights into the mechanisms of cell failure equivalent to that which could be obtained with a Li reference electrode inserted within the cell. The software is available free of charge by contacting the authors.
 [DOI: 10.1149/2.013209jes]

Manuscript submitted May 3, 2012; revised manuscript received June 11, 2012. Published August 14, 2012.

Li-ion batteries are widely used in cell phones, laptops and cameras due to their long life time and high energy density. However, Li-ion batteries need to have significantly longer life times in electric vehicles compared to portable electronics. The lifetime of a Li-ion cell depends on many factors, including the number of cycles, the charging current, the time since the beginning of use and the temperature history that the cell has experienced.

Smith et al.[1,2] showed that for the special case of low rate cycling (rates less than C/14) at elevated ($T \geq 30^{\circ}C$) temperature, the degradation rate of graphite/$LiCoO_2$, graphite/$LiFePO_4$ and graphite/$LiMn_2O_4$ cells was approximately independent of cycle number and primarily dependent on the time of exposure to high temperature during use. In such a situation, parasitic chemical reactions at the electrodes, which can be sensed by high precision coulometry, dominate compared to mechanical degradation of the electrodes and possible Li-plating at the negative electrode. In Reference 2, differential voltage analysis was effectively used to probe the degradation mechanisms.

In the general case of complex temperature profiles and charge and discharge currents it is important to be able to elucidate the causes of cell capacity loss. These can include loss of active mass at the positive or negative electrode, impedance increase and loss of active lithium due to continual solid electrolyte interphase (SEI) growth. Differential voltage analysis has been used effectively by several research groups to probe the reasons for cell failure.[3–5]

Differential voltage (dV/dQ vs. Q) measurements allow the features in the voltage vs. capacity data to be seen more clearly as shown in Figure 1. Figure 1a shows the voltage vs. capacity curves for a full Li-ion cell and the reference potential-capacity curves for the positive and negative electrodes measured versus Li/Li^+. The x-axis in Figure 1a is the total cell capacity, Q, (mAh) and has been calculated for the positive and negative reference curves by multiplying the specific capacity, q_p or q_n, by the appropriate electrode mass, m_p or m_n, and applying the appropriate electrode slippage, δ_p or δ_n, respectively. The potential vs. specific capacity curves for the individual electrodes were measured by taking the electrodes out of an identical full cell and making half cells with each electrode. Figure 1b shows the corresponding dV/dQ vs. Q curves where the features from the voltage vs. capacity and potential versus capacity curves are accentuated. The potential vs. specific capacity curves for the reference cells were measured at low rate (C/20) to ensure that the features are clear in the voltage curves and differential plots.

Observing changes in the dV/dQ curves with time allows for changes in the active masses, (m_p and m_n) and slippages (δ_p and δ_n) of the positive and negative electrodes to be determined. This is possible because dV/dQ vs. Q for a full cell can be calculated from dV_p/dq_p vs. q_p and dV_n/dq_n vs. q_n where $V_p(q_p)$ and $V_n(q_n)$ are the potential versus specific capacity of the reference electrodes. This is done using the following equation:

$$\frac{dV}{dQ}(Q) = \frac{1}{m_p}\frac{dV_p}{dq_p} - \frac{1}{m_n}\frac{dV_n}{dq_n} \qquad [1]$$

where $Q = q_p\, m_p + \delta_p$ and $Q = q_n\, m_n + \delta_n$. As a reminder, m_p is the active mass of the positive electrode in the Li-ion cell, m_n is the active mass of the negative electrode in the Li-ion cell and δ_p and δ_n are the positive and negative electrode slippages, respectively. Figure 1b illustrates the use of Eqn. 1 graphically and shows that dV/dQ vs. Q for the full cell is the superposition of the two differential voltage versus capacity curves from the reference electrodes, scaled by their masses and slipped appropriately.

User-Friendly Differential Voltage Analysis Freeware

A dV/dQ analysis software package has been written that facilitates the process described in Figure 1. The program takes a full cell voltage vs. capacity data set as well as two reference potential vs. capacity data sets and compares dV/dQ vs. Q from the full cell to dV/dQ vs. Q calculated from the two reference data sets using Eqn. 1. By matching the experimental and calculated dV/dQ vs. Q curves the user

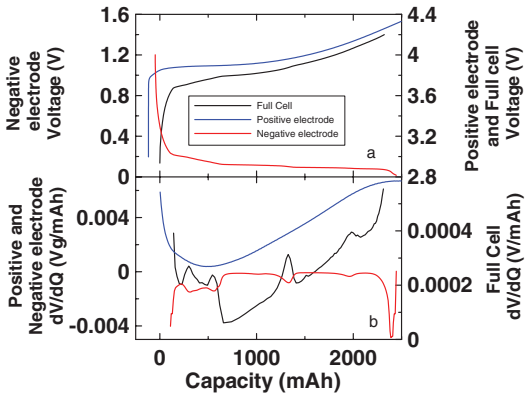

Figure 1. a) Voltage versus capacity of a full Li-ion cell (black – right axis), potential, V_p, versus capacity for the positive electrode (blue – right axis) and potential, V_n, versus capacity for the negative electrode (red – left axis). b) dV_p/dq_p (blue – left axis) and dV_n/dq_n (red – left axis) versus Q and dV/dQ vs. Q for the full cell (black – right axis).

*Electrochemical Society Student Member.
**Electrochemical Society Active Member.
zE-mail: jeff.dahn@dal.ca

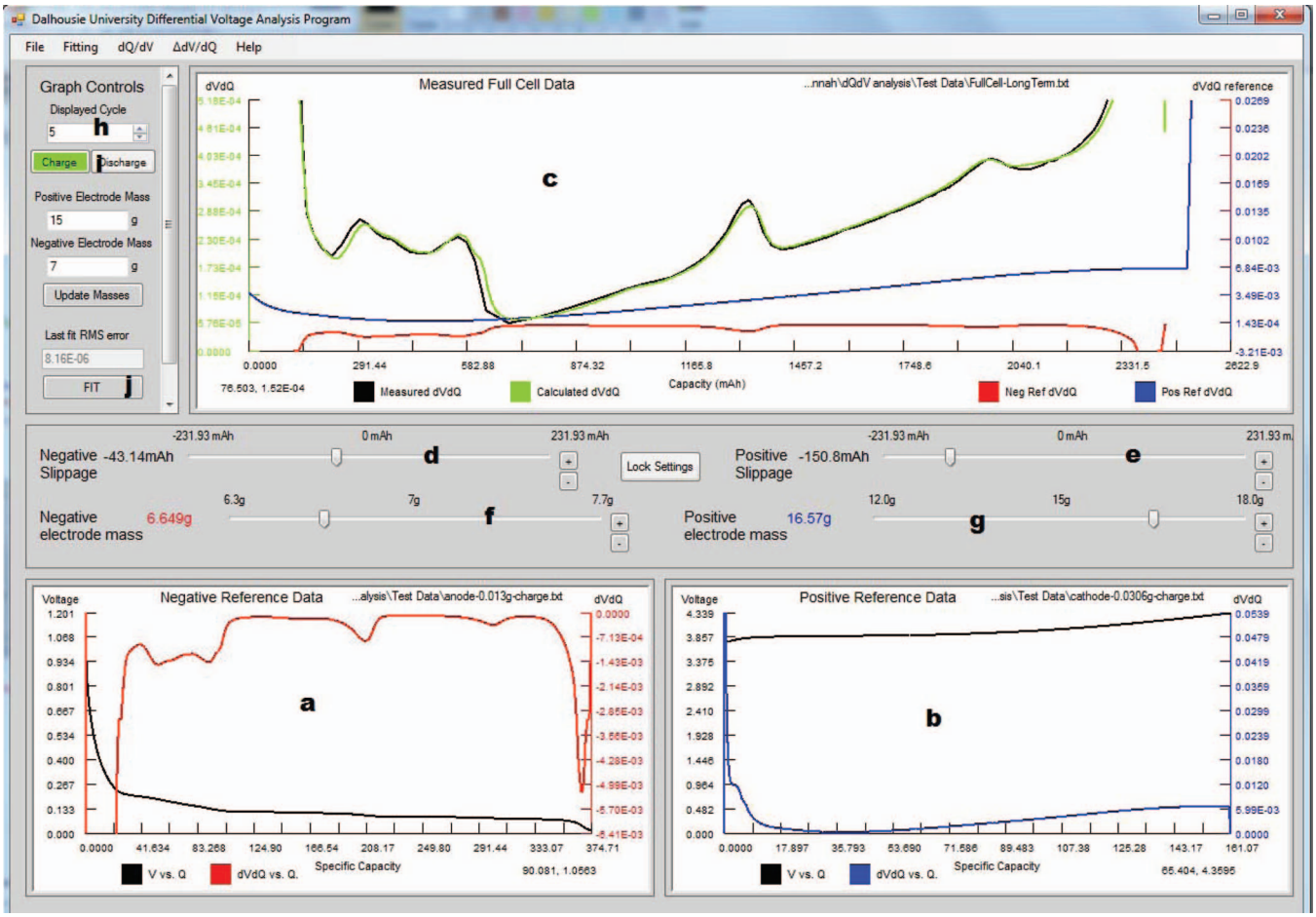

Figure 2. Screen shot of the dV/dQ analysis software. The letters a – j indicate program features as described in the text.

can obtain important information about the behavior of each electrode and a better understanding of cell degradation.

Program Structure and Operation.— The dV/dQ analysis program was written using Visual Basic.Net in Visual Basic Express 2010. The front panel, as seen in Figure 2, displays the measured full cell data and the reference cell data as well as various controls to manipulate the calculated dV/dQ vs. Q data. Program panel 2a displays voltage (V_n) vs. specific capacity (q_n) data and dV_n/dq_n vs q_n from one slow cycle of the negative electrode reference half cell. Ideally, this data should be collected at the same temperature and C-rate as the full cell data that is being described. Running the cells at $\leq$ C/20 is important to ensure that impedance does not influence the features in the voltage vs. capacity data. Program panel 2b displays the same information as panel 2a but for the positive electrode reference half cell. Program panel 2c displays dV/dQ vs. Q for one charge of the full cell as well as dV/dQ vs. Q calculated from the two reference curves and the four parameters m_p, m_n, δ_p and δ_n using Eqn. 1. Each of the parameters m_p, m_n, δ_p and δ_n is controlled by a slider as indicated by symbols g, f, e and d, respectively. Program panel 2c also shows dV_n/dQ vs. Q and dV_p/dQ vs. Q scaled by their active masses to facilitate manual adjustment of the sliders to get the best agreement between calculated and measured dV/dQ vs. Q curves.

Good quality commercially available battery testers can measure relatively noise-free dV/dQ vs. Q data. However, most chargers cannot keep track of the absolute cell capacity over many cycles due to imprecision in the currents, imprecision in the determination of the time at which the cell switches from charge to discharge, etc.[6] The High Precision Charger at Dalhousie University can accurately track the absolute cell capacity to an accuracy of 0.01% over 1 charge-discharge cycle, to 0.1% over ten cycles and to 1% over 100 cycles. Since this device is not universally available and since many of our own measurements are made with conventional chargers, it was decided that the differential capacity analysis software would use relative capacity on the horizontal axis of program panel 2c, not absolute capacity. Similar to Honkura et al.[5] relative capacity is measured from $Q = 0$ at the fully discharged state of each cycle. If a precision charger is used, the relative capacities of the full cell and positive and negative electrodes can be converted to absolute capacities. Then it is also possible to compare the positive and negative electrode slippages with those calculated by the dV/dQ vs. Q analysis software.

The front panel of the program illustrated in Figure 2 also includes controls that allow the user to increment the cycle number (see "h" in Figure 2) and switch between discharges and charges (see "i" in Figure 2). Reference data for charge or discharge must also be selected appropriately to match the charge or discharge of the full cell. There are also fitting capabilities available that are started with the fit button indicated as "j" in Figure 2. The fitting function uses a non-linear least squares fitting algorithm called the Levenberg-Marquardt method which is part of a data processing library from ALGLIB (www.alglib.net). The fitting function minimizes the least-squares difference between the measured and calculated dV/dQ vs. Q curves in program panel 2c by varying the four adjustable parameters m_p, m_n, δ_p and δ_n. All data points are normally weighted equally in the calculation of the least-squares difference. Linear interpolation between adjacent data points is used to ensure that the reference data and the full cell data have points at the same values of Q for the goodness of fit calculation. It may appear that the fitting function has only three degrees of freedom due to the constraints that come with Equation 1: $Q = q_p\, m_p + \delta_p$ and $Q = q_n\, m_n + \delta_n$. However, the additional condition

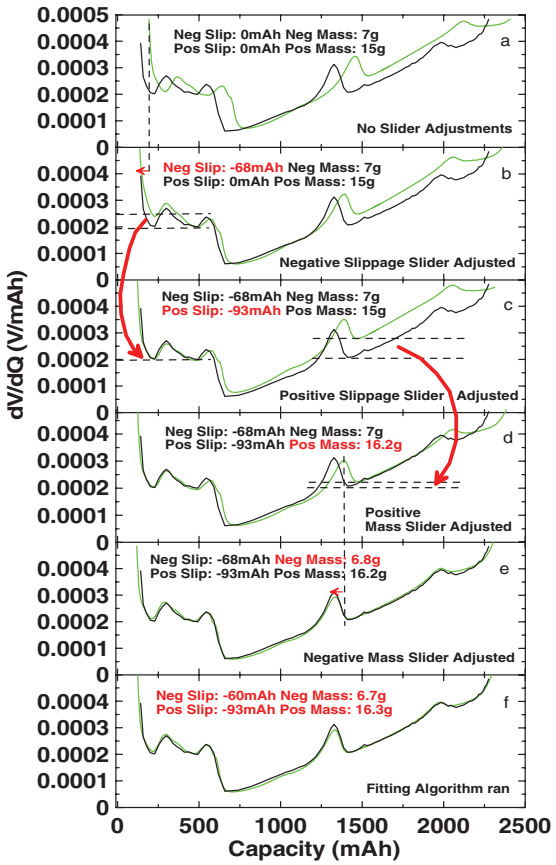

Figure 3. dV/dQ vs. Q for a graphite/$LiCoO_2$ Li-ion cell during operation of the dV/dQ analysis program. The black curve is the measured dV/dQ and the green curve is the calculated dV/dQ. As the panels progress from a to f, various adjustments to the calculations are made as indicated on the panels and in the text.

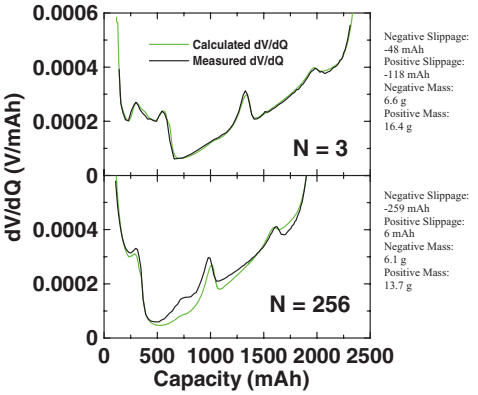

Figure 4. Measured and calculated dV/dQ vs. Q for a graphite/$LiCoO_2$ 18650-size cell at cycle 3 and at cycle 256. The cell was cycled at a rate of C/24 at 55°C for about 15 months.

$Q = 0$ in the fully discharged state uniquely defines the 4 parameters. The fitting function is capable of fitting the charge profile from a single cycle or the charge profile for all cycles of a given dataset. In the latter instance, the four parameters, m_p, m_n, δ_p and δ_n, are tabulated versus cycle number in an output file for later analysis by the researcher. The fitting function also has the option to using a weighting function that assigns higher priority to the fit of some parts of the data. The optional weighting factor is calculated as the absolute value of the second derivative with respect to Q of dV/dQ of the measured full cell data. This gives priority to fitting the various features in dV/dQ vs Q accurately. We do not normally employ this option.

Before using the fitting function the user must manually fit the data to obtain close agreement. Figure 3 demonstrates this procedure. Initially, Figure 3a, the calculated dV/dQ vs. Q curve does not match well with the measured full cell data. This is because the two slippage parameters are set at zero initially and the mass parameters are set at initial approximate guesses that are entered by the user. In Figure 3b, the negative slippage was adjusted so that the initial capacity of the calculated dV/dQ vs. Q curve lined up with the initial capacity of the measured full cell data. In Figure 3c, the positive slippage was adjusted so that the calculated dV/dQ vs. Q curve matched the height of the initial peak of the measured full cell data. In Figure 3d, the positive mass was increased which caused the right side of the calculated dV/dQ vs. Q data to better fit the measured full cell data. In Figure 3e, the negative mass was decreased which caused the middle peak of the calculated dV/dQ vs. Q data to align with the middle peak of the measured full cell data. Once the fit was reasonably close manually, the fitting function was run. Figure 3f shows the data and calculation after the fitting function was performed. The parameters were not changed dramatically but the fit was slightly better as observed during program operation in the "last fit RMS error" box. The usefulness of the program for reverse engineering commercial cells in the initial cycle should be obvious.

Examples of Program Use.— Figure 4 shows dV/dQ (V/mAh) vs. Q (mAh) for a commercial graphite/$LiCoO_2$ 18650 cell at the third cycle (Figure 4a) and after 256 cycles (Figure 4b). The cell was cycled using C/24 currents between 3.0 and 4.2 V at 55°C for roughly 15 months. The measured dV/dQ vs. Q is plotted along with the dV/dQ vs. Q values that were calculated by the dV/dQ analysis software from Li/graphite and Li/$LiCoO_2$ reference data. The electrodes in the half cell were identical to those used in the 18650 cell. The fit of the calculated data to the measured data is much better for the early cycle than for the later cycle, but the fit is still acceptable for the later cycle. There is a large change in both the positive and negative slippage as well as a decrease in both active masses. These changes can be examined more closely using Figure 5.

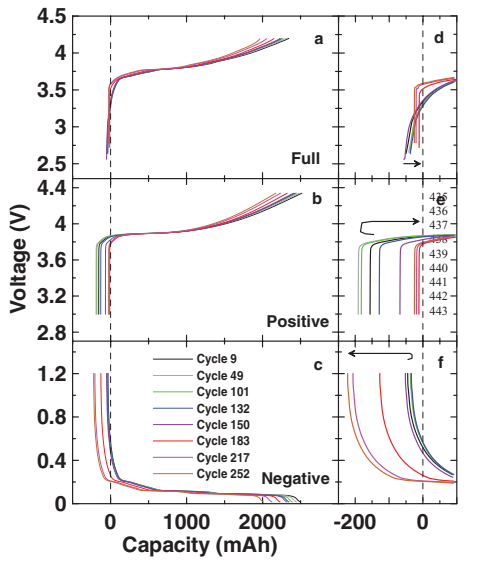

Figure 5. a) Calculated voltage versus relative capacity for a full graphite/$LiCoO_2$ cell at various cycles. b) V_p vs. Q for the positive electrode of the same cell as determined by the dV/dQ analysis program. c) V_n vs. Q for the negative electrode of the same cell as determined by the dV/dQ analysis program. $Q = 0$ represents the fully discharged state of the cell at each cycle. d–f) show expanded views near $Q = 0$. The positive and negative electrode slippages can be observed by the shifts of the V_p vs. Q and V_n vs. Q curves during cycling.

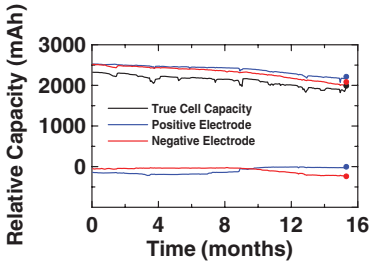

Figure 6. Full cell capacity (black) and end point capacities of the positive electrode (blue) and negative electrode (red) during the charge discharge cycling of a graphite/$LiCoO_2$ cell at C/24 and 55°C for a period of 15 months (see text).

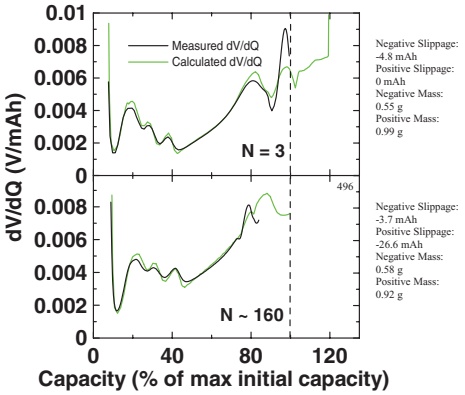

Figure 7. Measured and calculated dV/dQ versus % of max initial capacity for a wound graphite/$LiCoO_2$ cell at cycle 3 and at cycle 160 (see text). The values of the slippages and active electrode masses are listed to the right of each panel.

Figure 5 shows the voltage (V) vs. capacity (mAh) graphs for the full cell (Figure 5a) as well as the positive (Figure 5b) and negative electrode (Figure 5c) half cells for the same commercial graphite/$LiCoO_2$ cell described by Figure 4 over a number of different cycles. Using the fit parameters found using the dV/dQ analysis software, the voltage vs. capacity curves for the positive and negative electrodes have been shifted and scaled by the appropriate slippage and mass values. The slippage alterations caused a shift in the initial capacity of the voltage vs. capacity curves of the reference electrodes, which is shown clearly in the expanded views in Figures 5e and 5f. It is important to remember that the x-axis in Figure 5 is relative capacity: relative to Q = 0 at the bottom of discharge of the full cell where the graphite electrode has $|\delta_n|$ mAh of lithium remaining and the positive electrode can hold $|\delta_p|$ mAh of capacity before becoming full $LiCoO_2$. It may seem confusing that there is little shifting of the electrodes in the early cycles and then the positive electrode shifts to the right and the negative electrode shifts to the left. This behavior is explained in detail in Reference 2. Briefly, both electrodes slip to higher absolute capacity at similar rates during the early cycles. Then the slippage rate of the negative electrode slows due to the thickening of the SEI, while the positive electrode slippage continues which leads to the behavior shown in Figure 5.

The active mass changes cause a shrinking or expansion of the capacity range of the reference voltage vs. capacity curves. This is because the capacity of the negative and positive electrode that is plotted in Figure 5 is calculated from the specific capacity of the reference data multiplied by the active mass. Therefore, as the active mass decreases with cycle number so too does the total capacity of the positive and negative electrodes.

Figure 6 shows an alternative view of the results in Figure 5 for all cycles of the cell. Figure 6 shows the relative capacity (mAh) vs. time (months) for the positive electrode, negative electrode and full cell of the commercial graphite/$LiCoO_2$ cell described by Figure 5. The negative (red) and positive (blue) electrode curves have both an upper and lower limit of capacity, shown by two curves of the same color. For the negative reference electrode, these limits correspond to potentials of 0.0 and 1.5 V when the graphite is full and empty of lithium, respectively. For the positive reference electrodes, these limits correspond to potentials of 3.0 and 4.3 V when the Li_xCoO_2 is full and partly emptied of Li. The total cell capacity is given by the difference between the black curve (charge capacity) and 0, since the capacity of the cell in the discharged state is Q = 0. Figure 6 shows that for the first 9 months of testing, when the cell is fully discharged (Q = 0), the negative electrode is nearly empty and the positive electrode is not completely filled. However, after 9 months, the limit of discharge is determined when the positive electrode is completely filled with lithium. Figure 6 also shows that in the fully charged state of the cell (4.2 V) the graphite negative electrode is not completely filled with Li (capacity of the black curve is always less than that of the upper red curve) at any time and that the positive electrode never reaches 4.3 V vs. Li/Li^+ (capacity of the upper blue curve is always greater than the black curve). The details of Figure 6 are explained in greater detail in Reference 2.

Figure 7 shows dV/dQ (V/mAh) vs. capacity (% max capacity) for a different wound graphite/$LiCoO_2$ cell. This cell was cycled 20 times at 40°C using a current corresponding to C/20 on the High Precision Charger at Dalhousie University between 3.4 and 4.075 V. Then it was cycled 140 times at 55°C on a traditional charger using a current corresponding to C/12 between the same potential limits. Then the cell was placed back on the High Precision Charger at 50°C for further cycling at C/50 to collect data suitable for dV/dQ analysis. This cell had an electrolyte of 1M $LiPF_6$ EC:EMC (3:7) with no electrolyte additives. Figure 7a shows the measured and calculated dV/dQ vs. Q for cycle 3 and Figure 7b shows the same information for cycle 160. The agreement between measured and calculated dV/dQ vs. Q in Figure 7 is not as impressive as in Figure 4. This is because the cell studied in Figure 7 is a small wound cell with a negative electrode overhang which represents more than 10% of the negative electrode width. This means that the negative electrode reference curve does not exactly describe what is happening in the negative electrode of the full cell due to partial utilization of the material in the overhang region.

The fitted values shown to the right of the graphs in Figure 7 show that a large shift in positive electrode slippage and a decrease in positive electrode active mass have occurred between the two cycles. There is also what appears to be a small increase in negative active mass which is caused by the fact that the latter cycle was measured at 50°C while the earlier cycle was measured at 40°C: the overhang in the negative electrode is better utilized at the higher temperature. The electrolyte resistance has decreased at the higher temperature and therefore reactions are capable of extending further into the electrode overhang and more active material is functional.

The dV/dQ analysis software can also be used to assess the impact of electrolyte additives on the behavior of cells. Figure 8 shows the voltage (V) vs. capacity (% max capacity) curves for the positive electrode, negative electrode and full cell of three wound graphite/$LiCoO_2$ cells (same type of cell as in Figure 7) at an early cycle and after about 160 cycles. These cells were cycled under the same temperature-rate regime as the cell described by Figure 7. Figure 8a shows the voltage vs. capacity curves for a cell with no electrolyte additives. Figure 8b and Figure 8c show the voltage vs. capacity curves for cells with 1% VC and 2% VC additives to the 1M $LiPF_6$ EC:EMC (3:7) base electrolyte, respectively. Figure 8 shows that the addition of VC decreases the amount of positive electrode slippage when the curves are plotted versus relative capacity. Alternatively, it can be stated that the addition of VC reduces the relative slippage between the electrodes which leads to improved capacity retention. Figure 8 shows that the negative electrode grows in capacity from the early to the late cycle. This is due to the increase in temperature, as described above, that causes more active material in the overhang region to be accessed due to decreased electrolyte resistance. Figure 8 shows that the total

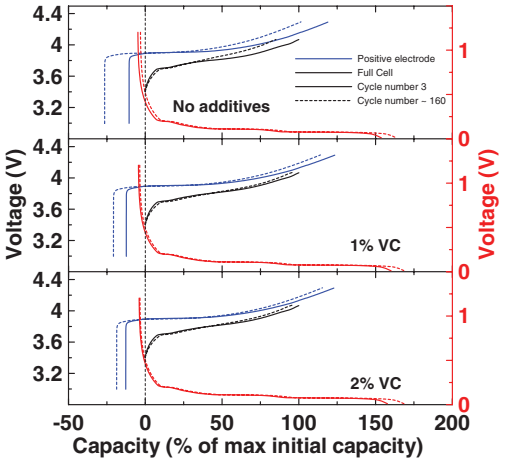

Figure 8. Calculated full cell voltage, positive electrode potential and negative electrode potential versus % of max initial capacity for wound graphite/$LiCoO_2$ cells. Results are shown for cycle 3 and a cycle near cycle 160. The relative electrode slippages that occur during cycling are easily discerned from this Figure. top) no electrolyte additives; middle) 1% VC additive and bottom) 2% VC additive.

capacity of the negative electrode is much larger than that of the positive electrode and the full cell in the particular design used in these cells. This indicates that there is an excess of negative electrode in these cells. Observations such as this can be used to reverse engineer cell characteristics such as the N:P ratio.

The reader is cautioned that the graphs in Figure 8 may leave an impression that the positive electrode undergoes negative absolute slippage during cycling. This is not the case. The reader must always remember that $Q = 0$ is always taken as the capacity of the fully discharged full cell which removes the absolute slippage (which most chargers cannot measure) from the data. When the absolute slippage is added (see Ref. 2) both electrodes slip to greater capacities and the graphite slips faster than the positive electrode, so in the presentation of Figure 8, the positive electrode has negative slippage relative to the graphite since the graphite is almost stationary relative to $Q = 0$.

Access to program.— The dV/dQ analysis program executable code and reference electrode data set library can be obtained by contacting the authors. The reference electrode data set library contains data for several graphite samples measured at various rates and temperatures as well as data for common positive electrode materials like $LiCoO_2$, $Li[Ni_{0.80}Co_{0.15}Al_{0.05}]O_2$, $Li_{1+x}Mn_{2-x}O_4$ and $Li[Ni_{0.42}Mn_{0.42}Co_{0.16}]O_2$. Updates to the reference electrode data set are ongoing.

Conclusion

A user-friendly dV/dQ vs. Q analysis program has been developed in VB.NET software compatible with the Windows platform. This software is very useful in understanding the degradation that occurs in Li-ion batteries during cycling. As shown in Figures 5 and 8, the results of the application of the software are equivalent to results that could be obtained with a reference electrode placed in the Li-ion cell. The software is available for free by contacting the authors.

Acknowledgments

This work was funded by the NSERC/3M Canada Industrial Research Chair program in Materials for Advanced Batteries.

References

1. A. J. Smith, J. C. Burns, X. Zhao, D. Xiong, and J. R. Dahn, *J. Electrochem. Soc.*, **158**, A447 (2011).
2. A. J. Smith, Hannah M. Dahn, J. C. Burns, and J. R. Dahn, *J. Electrochem. Soc.*, **159**, A705 (2012).
3. I. Bloom, J. P. Christophersen, D. P. Abraham, and K. L. Gering, *J. Power Sources*, **157**, 537 (2006).
4. I. Bloom, A. N. Jansen, D. P. Abraham, J. Knuth, S. A. Jones, V. S. Battaglia, and G. L. Henriksen, *J. Power Sources*, **139**, 295 (2005).
5. K. Honkura, H. Honbo, Y. Koishikawa, and T. Horiba, *ECS Transactions*, **13**, 61 (2008)
6. A. J. Smith, J. C. Burns, S. Trussler, and J. R. Dahn, *J. Electrochem. Soc.*, **157**, A196 (2010).